

# Measurement of splittings along a jet shower in $\sqrt{s} = 200 \text{ GeV } pp$ collisions at STAR

Raghav Kunnawalkam Elayavalli<sup>1,2</sup> for the STAR Collaboration

<sup>1</sup> Wright Laboratory, Yale University

<sup>2</sup> Brookhaven National Laboratory

raghav.ke@yale.edu

July 29, 2021



*Proceedings for the XXVIII International Workshop  
on Deep-Inelastic Scattering and Related Subjects,  
Stony Brook University, New York, USA, 12-16 April 2021  
doi:10.21468/SciPostPhysProc.?*

1

## 2 Abstract

3 Jets are algorithmic proxies of hard scattered partons, i.e. quarks and gluons, in high  
4 energy particle collisions. The STAR collaboration presents the first measurements of  
5 substructure observables at the first, second and third splits in the jet clustering tree via  
6 the iterative SoftDrop procedure. For each of these splits, we measure the fully corrected  
7 groomed shared momentum fraction ( $z_g$ ) and groomed jet radius ( $R_g$ ). We discuss the  
8 evolution of jet substructure in both the angular and momentum scales which allows for  
9 a self-similarity test of the DGLAP splitting function. We compare the fully corrected data  
10 to Monte Carlo models, providing stringent constraints on model parameters related to  
11 the parton shower and non-perturbative effects such as hadronization.

## 12 1 Introduction

13 Jets are composite objects resulting from a convolution of parton shower (perturbative-QCD)  
14 and fragmentation (non-perturbative-QCD) processes, and as such they contain rich substructure  
15 information that can be exploited via jet finding algorithms [1]. These algorithms typically  
16 employ an iterative clustering tree procedure that generates a tree-like structure, which upon  
17 an inversion, gives access to jet substructure at different steps along the cluster tree. The most  
18 common toolkit for such measurements is SoftDrop [2] which employs a Cambridge/Aachen  
19 re-clustering of jet constituents and imposes a criterion at each step as we walk backwards in  
20 the de-clustered tree,

$$z_g = \frac{\min(p_{T,1}, p_{T,2})}{p_{T,1} + p_{T,2}} > z_{\text{cut}} \left( \frac{R_g}{R_{\text{jet}}} \right)^\beta ; R_g = \Delta R(1, 2), \quad (1)$$

21 where 1, 2 are the two prongs at the current stage of de-clustering,  $p_T$  is the transverse momen-  
22 tum of the respective prong,  $R_{\text{jet}}$  is the jet resolution parameter and  $\Delta R$  is the radial distance  
23 in the pseudorapidity  $\eta$ -azimuthal angle( $\phi$ ) plane. The free parameters in Eq. 1 are  $z_{\text{cut}}$  a  
24 momentum fraction threshold, and  $\beta$ , the angular exponent which in our analysis are set to  
25 0.1 and 0, respectively [3]. These parameter values make SoftDrop observables calculable in  
26 a Sudakov-safe manner, and at the infinite jet momentum limit they converge to the DGLAP

27 splitting functions. STAR recently measured the SoftDrop groomed shared momentum frac-  
 28 tion ( $z_g$ ) and groomed jet radius ( $R_g$ ) at the first surviving split for jets of varying transverse  
 29 momenta and jet radii [4]. These double differential measurements were fully corrected in  
 30 both jet  $p_T$  and  $z_g/R_g$  simultaneously. The data demonstrate a significant variation in  $R_g$  as  
 31 the  $p_{T,\text{jet}}$  increases, reflecting momentum dependent narrowing of jet substructure, whereas  
 32  $z_g$  only varies slowly and has a relatively constant shape for  $p_{T,\text{jet}} > 30$  GeV/c.

33 Since the jet clustering tree extends beyond the first split, we iteratively apply the SoftDrop  
 34 procedure on the hardest (highest  $p_T$ ) surviving branch and measure the jet substructure at  
 35 each split along the de-clustered tree [5]. Such measurements enable, for the first time, a  
 36 time-differential study of the parton shower and evolution of both the momentum ( $z_g$ ) and  
 37 angular scales ( $R_g$ ) within a jet. Upon applying the iterative SoftDrop procedure, with the  
 38 same aforementioned values of the parameters, we reconstruct a collection of observables  
 39 corresponding to  $z_g^n$  and  $R_g^n$  at a given split  $n$ . We limit our measurement to the first three  
 40 surviving splits within each jet and present the results fully corrected in 3-D corresponding to  
 41 the jet or initiator  $p_T$ ,  $z_g/R_g$ , and the split number  $n$  for jets of varying  $p_{T,\text{jet}}$  and for splits of  
 42 varying initiator  $p_T$ . This provides the potential benefit of studying the self-similarity of the  
 43 QCD splitting functions.

## 44 2 Analysis details

45 The  $pp$  data utilized in this measurement was collected with the STAR detector [6] during the  
 46 2012 run at  $\sqrt{s} = 200$  GeV. Events are selected by an online jet patch trigger in the Barrel Elec-  
 47 troMagnetic Calorimeter (BEMC) which is a  $1 \times 1$  patch in  $\eta \times \phi$  with a total sum  $E_{T,\text{patch}} > 7.3$   
 48 GeV. Events are also required to have their primary vertices, reconstructed via charged particle  
 49 tracks from the Time Projection Chamber (TPC), to be within  $|v_z| < 30$  cm along the beam axis  
 50 from the center of the detector. Jets are reconstructed from charged tracks ( $0.2 < p_T < 30.0$   
 51 GeV/c) in the TPC and energy depositions in the BEMC towers ( $0.2 < E_T < 30.0$  GeV) using  
 52 the anti- $k_T$  algorithm with a resolution parameter  $R_{\text{jet}} = 0.4$  as implemented in the FastJet  
 53 package [7]. Same track, tower and jet selections are applied as in [4].

54 A novel correction technique is employed for this 3-D measurement. Detector smearing  
 55 effects on the substructure observables  $z_g$  and  $R_g$  at a given split, and at a given initiator  $p_T$  or  
 56 jet  $p_T$  are unfolded via a 2-D Iterative Bayesian procedure as implemented in the RooUnfold  
 57 package [8]. The detector response is estimated via PYTHIA 6 (Perugia 2012 tune [9] and  
 58 further tuned to STAR data [10]) events passed through a GEANT3 simulation of the STAR de-  
 59 tector. These simulated events are embedded into zero-bias  $pp$  data and the resulting events  
 60 are analyzed in a similar fashion to the real data. Since the splits are identified at the detector  
 61 level, detector effects on the jet clustering tree could mangle the split hierarchy, i.e. splits at  
 62 the particle level can be lost or mis-categorized in the detector-jet clustering tree, along with  
 63 the addition of fake splits arising from particles of uncorrelated sources, such as interactions  
 64 with detector material. To correct the split hierarchy, we introduce an additional matching  
 65 requirement of the splits based on the initiator prong at the particle and detector-level via  
 66  $\Delta R(\text{initiator}_{\text{det,part}}) < 0.1$  to build a hierarchy matrix with particle-level splits on the  $x$ -axis  
 67 and detector-level splits on the  $y$ -axis. The 2-D unfolded data are then added with the rele-  
 68 vant weights along each column of the hierarchy matrix to get a fully corrected particle-level  
 69 distribution of  $z_g$  and  $R_g$  as a function of the jet/initiator  $p_T$  at a true split  $n$ .

70 The systematic uncertainties follow the same procedure outlined in [4], and are broadly  
 71 grouped into two categories: detector performance and analysis procedure. The former sources  
 72 of uncertainties constitute variations of the tracking efficiency by  $\pm 4\%$  and tower energy scale  
 73 by  $\pm 3.8\%$ . The systematic uncertainty due to the analysis procedure includes hadronic correc-

74 tion, i.e. correcting 100% to 50% of the matched track's momentum from a tower's energy to  
 75 negate double counting of energy depositions. Uncertainty due to the unfolding procedure is  
 76 taken as the maximal envelope of variations in the iteration parameter and shape uncertain-  
 77 ties arising from the prior (varied by the differences to PYTHIA 8 [11] and HERWIG 7 [12]).  
 78 Lastly, the split matching criterion is varied by  $\pm 0.025$  and the consequent variation to the  
 79 fully corrected result is taken as a shape uncertainty.

### 80 3 Results

81 The fully corrected data are shown in Fig. 1 for the first, second and third splits as black, red  
 82 and blue colored markers, respectively, and the shaded regions around data markers repre-  
 83 sent the total systematic uncertainty. The top panels show  $z_g$  for two different initiator  $p_T$   
 84 selections,  $[20, 30]$  GeV/c on the left and  $[30, 50]$  GeV/c on the right, and the bottom pan-  
 85 els show  $R_g$  for two jet  $p_T$  selections. These measurements exhibit a remarkable feature of  
 86 substructure evolution along the jet shower, e.g. a gradual variation in both  $z_g$  and  $R_g$  as we  
 87 move from the first to the third splits. The  $R_g$  at a split can be interpreted as the available  
 88 phase space for subsequent emissions/splits, and is also related to the virtuality at the split.  
 89 As  $R_g$  gets progressively narrower with increasing split  $n$ , the shape of the  $z_g$  also changes from  
 90 being sharply peaked at smaller values, i.e. asymmetric splitting, to a flatter distribution with  
 91 increased probability for symmetric splits.

92 In comparing the left and right panels of Fig. 1, a weak dependence on the jet/initiator  
 93  $p_T$  is observed, while the phase space restrictions via selecting a split (first, second or third)  
 94 significantly impacts the substructure observables.

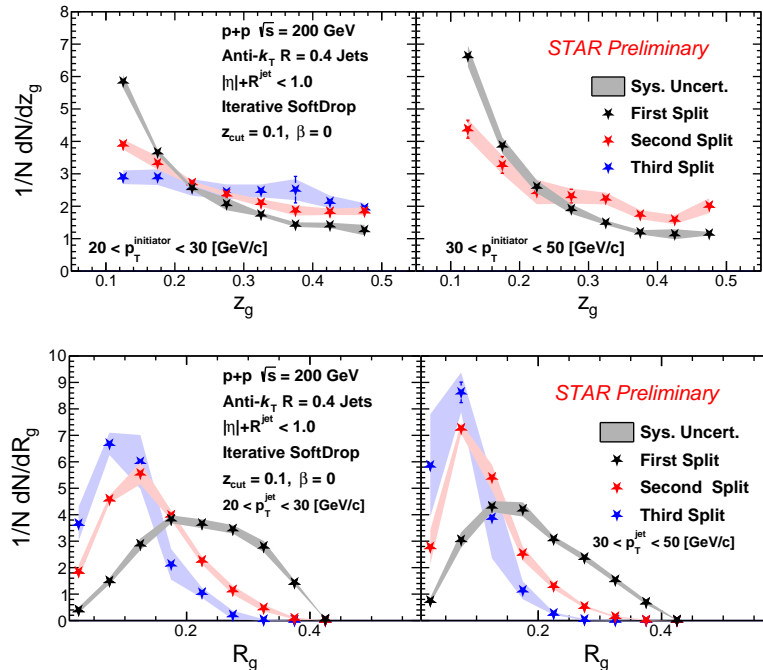


Figure 1: Measurements of the iterative SoftDrop splitting observables,  $z_g$  (top panels) and  $R_g$  (bottom panels), for the first (black markers), second (red markers) and third (blue markers) splits. The top (bottom) panels are differential in initiator (jet)  $p_T$  for two selections corresponding to  $20 < p_T < 30$  (left) and  $30 < p_T < 50$  (right) GeV/c.

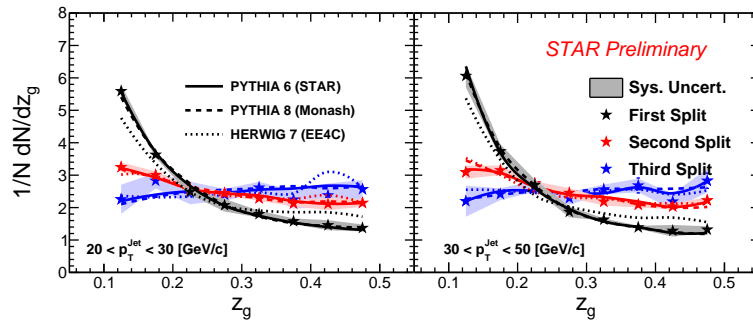


Figure 2: Iterative SoftDrop  $z_g$  for first, second and third splits for various  $p_{T,\text{jet}}$  selections (left and right) compared to predictions from PYTHIA 6 (solid line), PYTHIA 8 (dashed) and HERWIG 7 (dotted) event generators.

95 Figure 2 shows the fully unfolded  $z_g$  for the first (black), second (red) and third (blue)  
 96 splits for  $20 < p_{T,\text{jet}} < 30$  (left) and  $30 < p_{T,\text{jet}} < 50$  (right) GeV/c compared with leading  
 97 order monte carlo (MC) event generators PYTHIA 6 (solid), PYTHIA 8 (dashed) and HERWIG  
 98 7 (dotted). The MC models are able to reproduce the evolution of  $z_g$  as we increase the split  $n$ .  
 99 The slight differences observed for the HERWIG predictions at the first split vanish for higher  
 100 splits, where one expects a greater impact of non-perturbative corrections.

## 101 4 Conclusion

102 STAR has measured the fully corrected iterative SoftDrop  $z_g$  and  $R_g$  distributions for the first,  
 103 second and third splits along the jet clustering tree. These measurements are presented as  
 104 a function of both the jet  $p_T$  and the initiator  $p_T$ . We observe a significant modification of  
 105 the shape of  $z_g$  and  $R_g$  as we travel along the jet shower from the first to the third splits due  
 106 to a constriction of the available phase space for radiations. Such an evolution can be con-  
 107 nected to the jet's virtuality and its subsequent evolution from hard scattering scale ( $Q^2$ ) to  
 108 the hadronization scale ( $\Lambda_{\text{QCD}}$ ). The fully corrected data are compared to leading order MC  
 109 event generators which showcase an overall qualitative agreement with the data albeit slight  
 110 differences at the first split which are reduced for second and third splits. In the near future,  
 111 the data will be compared to MC generators with varying perturbative (parton showers) and  
 112 non-perturbative (hadronization, multi-parton interactions) implementations to highlight the  
 113 transition between the two regions of the jet shower. This technique opens up the exciting pos-  
 114 sibility of space-time tomography in Au+Au collisions and enables differential measurements  
 115 of jet energy loss for specific substructure.

## 116 References

- 117 [1] S. Marzani, G. Soyez and M. Spannowsky, Lect. Notes Phys. **958**, pp. (2019)  
 118 [2] A. J. Larkoski, S. Marzani, G. Soyez and J. Thaler, JHEP **05**, 146 (2014)  
 119 [3] A. J. Larkoski, S. Marzani and J. Thaler, Phys. Rev. D **91**, no.11, 111501 (2015)  
 120 [4] J. Adam *et al.* [STAR], Phys. Lett. B **811**, 135846 (2020)  
 121 [5] F. A. Dreyer, L. Necib, G. Soyez and J. Thaler, JHEP **06**, 093 (2018)

- 122 [6] K. H. Ackermann et. al., Nucl. Instrum. Methods Phys. Res., Sect. A 499, (2003) 624
- 123 [7] M. Cacciari, G. P. Salam, and G. Soyez, J. High Energy Phys. 04 (2008) 005.
- 124 [8] G. D'Agostini, Nucl. Instrum. Meth. A **362**, 487-498 (1995) doi:10.1016/0168-  
125 9002(95)00274-X
- 126 [9] T. Sjostrand, S. Mrenna and P. Z. Skands, JHEP **05**, 026 (2006) doi:10.1088/1126-  
127 6708/2006/05/026 [arXiv:hep-ph/0603175 [hep-ph]].
- 128 [10] J. Adam *et al.* [STAR], Phys. Rev. D **98**, no.3, 032011 (2018)  
129 doi:10.1103/PhysRevD.98.032011 [arXiv:1805.09742 [hep-ex]].
- 130 [11] T. Sjöstrand, S. Ask, J. R. Christiansen, R. Corke, N. Desai, P. Ilten, S. Mrenna, S. Pres-  
131 tel, C. O. Rasmussen and P. Z. Skands, Comput. Phys. Commun. **191**, 159-177 (2015)  
132 doi:10.1016/j.cpc.2015.01.024 [arXiv:1410.3012 [hep-ph]].
- 133 [12] J. Bellm, S. Gieseke, D. Grellscheid, S. Plätzer, M. Rauch, C. Reuschle, P. Richardson,  
134 P. Schichtel, M. H. Seymour and A. Siódmok, *et al.* Eur. Phys. J. C **76**, no.4, 196 (2016)  
135 doi:10.1140/epjc/s10052-016-4018-8 [arXiv:1512.01178 [hep-ph]].